Mass-Energy Relations in the Fission of Highly Excited Heavy Nuclei*

ELDON L. HAINES† AND STANLEY G. THOMPSON
Lawrence Radiation Laboratory, University of California, Berkeley, California
(Received 22 April 1963)

Mass-energy relations in the fission of the compound nucleus Fm^{254} have been studied at excitation energies in the range from 58 to 116 MeV. This compound nucleus was produced by bombardments of Th^{232}, U^{238}, and Pu^{242} with the heavy ions Ne^{22}, O^{16}, and C^{12}, respectively. The kinetic energies of the two fission fragments from each event were measured by using semiconductor detectors. From these energies the masses and total kinetic energies were calculated.

The mass distributions were studied as a function of the total kinetic energy. The bell-shaped mass distributions narrowed rapidly as the kinetic energies of the fragments increased. The quantitative behavior of this narrowing suggests that most of the initial excitation energy of the compound nucleus is not available either for conversion into kinetic energy of the fragments or for the production of asymmetric mass divisions that are energetically unfavorable.

I. INTRODUCTION

WHEN elements heavier than radium are bombarded with charged particles, the most probable reaction is binary fission. The probability that a compound nucleus will de-excite to its ground state by particle emission is very small. If the projectiles are protons, deuterons, or α particles, direct interactions may compete actively with compound-nucleus formation. The resulting fission occurs at a wide variety of excitation energies, which makes interpretation of the data difficult and ambiguous.

It is well known that at low-excitation energies these heavy elements fission asymmetrically. As the excitation energy is increased, symmetric fission begins to compete favorably with asymmetric fission.[1] Until recently, the study of mass distributions of fission products at high, well-defined excitation energies has not been possible.

Use of heavy-ion accelerators has made possible very high, well-defined excitation energies. Although a 160-MeV O^{16} ion, for example, has the same velocity as a 40-MeV α particle, much greater excitation can be introduced in a reaction by the O^{16} ion without increasing the probability for direct interactions.

A study of mass-energy relations in the fission of highly excited heavy nuclei is reported here. The compound nucleus studied was Fm^{254}, with excitation energies ranging from 58 to 116 MeV. This compound nucleus was created in the following three ways: (a) $C^{12}+Pu^{242}$; (b) $O^{16}+U^{238}$; and (c) $Ne^{22}+Th^{232}$. The experiments involved measurement of the kinetic energies of the two fission fragments for each event. From conservation of linear momentum and conservation of mass, the masses of the fragments were determined. The variations of the mass distributions with total kinetic energy were studied by the method of moments.

II. EXPERIMENTAL

A. Equipment

1. *Heavy-Ion Beams*

Heavy ions having energies corresponding to 10 MeV per nucleon were supplied by the Berkeley heavy-ion linear accelerator (Hilac).[2] To reduce energies of the heavy ions to the desired values, aluminum foils of known thickness were placed in the beam path between two collimators. The foil thickness required for a given energy degradation was determined from Northcliffe's range-energy curves for heavy ions.[3]

2. *Fission Chamber*

The fission chamber, approximately 60 cm in diameter, had two detector arms whose angular positions could be adjusted from outside the chamber (Fig. 1). In addition, the radial position of each detector and the amount of absorber in the beam path could be controlled without opening the chamber. The target mount extended through the top of the chamber, making the

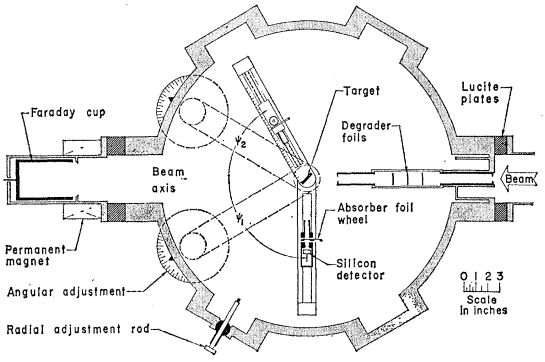

FIG. 1. Fission chamber. In the experiments described here, the detector located at angle ψ_2 was larger than that shown in the figure. Thus, it could detect all fission fragments in coincidence with those striking the detector at the angle ψ_1.

* This work was done under the auspices of the U. S. Atomic Energy Commission.
† Present address: Department of Chemistry, Purdue University, Lafayette, Indiana.
[1] Earl K. Hyde, Lawrence Radiation Laboratory UCRL-9065, 1960 (unpublished), pp. 7a, 27, 57, and 59.
[2] E. L. Hubbard, W. R. Baker, K. W. Ehlers, H. S. Gordon, R. M. Main, *et al.*, Rev. Sci. Instr. **32**, 621 (1961).
[3] L. C. Northcliffe, Phys. Rev. **120**. 1744 (1960).

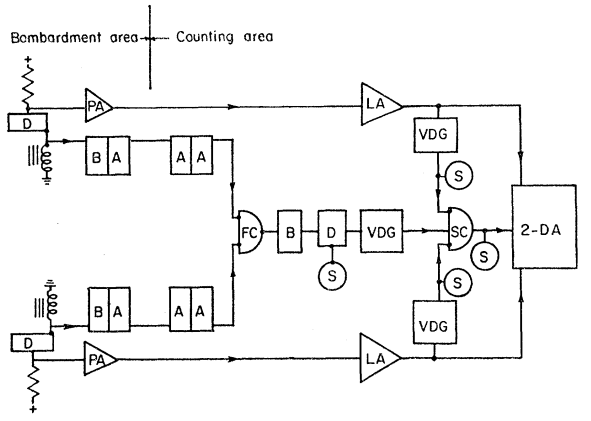

FIG. 2. Electronic system. The n-type side of the detectors is connected to the positive bias. The components include (D) 150-Ω-cm surface-barrier detectors (see Ref. 5), (PA) Model-VI pre-amplifiers (see Ref. 7), (LA) Model-VI linear amplifiers (see Ref. 7), (B) HP-460B inverting distributed amplifiers (see Ref. 8), (A) HP-460A noninverting distributed amplifiers (see Ref. 8), (FC) a fast-coincidence unit (see Ref. 8), (DS) a 10-Mc/sec discriminator (see Ref. 8), (VDG) variable-delay-and-gate units, (SC) a slow-coincidence unit, (S) scalers, and (2-DA) a two-dimensional analyzer.

target angle adjustable from outside. A permanent magnet at the mouth of the Faraday cup prevented electrons from entering or leaving the cup. Two vertical beam collimators (2 by 6 mm) were placed 60 cm apart, with the second one 5 cm from the target.

3. *Electronic System*

Gold surface-barrier detectors, similar to those described by Blankenship, were used for detection of the fragments and measurement of their energies.[4,5] For most measurements, 13/16-in.-diam detectors made from 150-Ω-cm n-type silicon were used. These gave linear calibration curves when operated at reverse biases of 3 to 6 V. Judged by their response to the single-fragment energy spectrum of Cf^{252}, the detectors showed good energy resolution.[6]

The electronic system (Fig. 2) was composed of three interdependent parts. The linear systems amplified the pulses from each detector for pulse-height analysis.[7] The coincidence system time-resolved the pulses.[8] Only pulses appearing within 10^{-8} sec of one another were accepted. Finally, a two-dimensional analyzer, activated by the coincidence system, measured the two linear pulse heights and stored the results on magnetic tape.

4. *Targets*

The Pu^{242} and Th^{232} targets[4] were prepared by electrodepositing the metal oxides onto thin nickel foils. A 250-$\mu g/cm^2$-thick Pu target was used in these experiments; the Th target thickness was 300 $\mu g/cm^2$. The U^{238} target, prepared by vaporization of UF_4, was 110 $\mu g/cm^2$ thick. The thickness of these targets was found by measuring the alpha decay rate from a known area. The Au^{197} target used for calibrating the linear systems was 400 $\mu g/cm^2$ thick. Its thickness was determined by the amount it degraded the energies of fragments from the spontaneous fission of Cf^{252}.

B. Bombardment Procedures

1. *Calibration of the Linear Systems and the Two-Dimensional Analyzer*

Calibration of the linear systems depended on the fact that fragments from heavy-ion-induced fission have higher energies when observed at forward angles than at backward angles. The high momentum of the energetic heavy ion imparts a high velocity to a fissioning nucleus. This velocity becomes a component of each fragment's laboratory (lab) velocity, causing its lab energy to be dependent on the lab angle. Fission-fragment pulse-height spectra from the system O^{16} (165 MeV)+Au^{197} were observed at angles of 140, 110, 90, 70, and 40 deg. (Angle ψ in Fig. 1.) The peak positions of these spectra plotted against the calculated lab energies constituted a calibration from 43 to 103 MeV (Fig. 3).[4]

2. *Data Collection*

Calculation of center-of-mass (c.m.) energies required a knowledge of the lab energies and one lab angle. Thus, it was necessary to define the lab angle by collimating one detector. Collimation to an arc of 4 deg

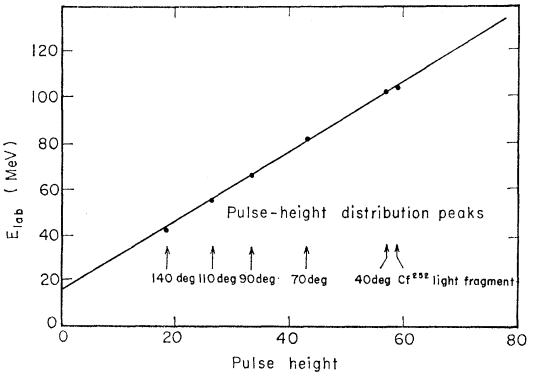

FIG. 3. Calibration of a linear system by using the angular variation of O^{16}(165 MeV)+Au^{197} fission-fragment energies. The Cf^{252} light-fragment peak is also included.

[4] For details of experimental techniques, calculations, and analysis of errors, see Eldon L. Haines, Lawrence Radiation Laboratory Report UCRL-10342, 1962 (unpublished).

[5] J. L. Blankenship, in *Semiconductor Nuclear Particle Detectors, Proceedings of an Informal Conference*, edited by J. S. T. Dabbs and F. J. Walter (National Academy of Sciences-National Research Council, Washington, D. C., 1961), Publication No. 871.

[6] H. C. Britt and H. E. Wegner, Rev. Sci. Instr. 34, 274 (1963).

[7] William W. Goldsworthy, Lawrence Radiation Laboratory Report UCRL-9816, 1961 (unpublished).

[8] Lawrence Radiation Laboratory Counting Handbook UCRL-3307 Rev., 1959 (unpublished).

made the calculation fairly accurate, yet allowed data collection to proceed at a reasonable rate. This collimated detector was usually located at 90 deg (lab). The second detector had a sufficient width (20 deg of arc) to accept all the fragments in coincidence with those striking the collimated detector. Previously measured angular correlations indicated what the angular location of the second detector should be.[9]

The limiting factor in the data-collection rate was the counting rate in the larger detector. The intensities of the particle beams were adjusted to limit the overlapping of linear pulses from the larger detector to less than 2%. When beam and target conditions were optimum, as many as 100 000 events were collected in a single experiment. With less favorable conditions, as few as 20 000 events were collected.

III. CALCULATIONS

A. Transformations

Fission-fragment lab energies were assigned to the pulse heights from two linear calibration curves.[4] An example of such a calibration curve is shown in Fig. 3. The corresponding c.m. energies, E_1 and E_2, were calculated from these two lab energies and the lab angle of the collimated detector.

The total kinetic energy of a fission event is given simply by

$$E_K = E_1 + E_2.$$

Using the conservation of linear momentum and assuming that the sum of the fragment masses, A_1 and A_2, equals the mass of the compound nucleus, A_c, we may calculate the fragment mass,

$$A_2/A_c = E_1/(E_1+E_2).$$

Here the fragment mass is expressed as a dimensionless fraction of the mass of the compound nucleus. The above relation is an approximation to the extent that any effects due to neutron emission have been neglected.

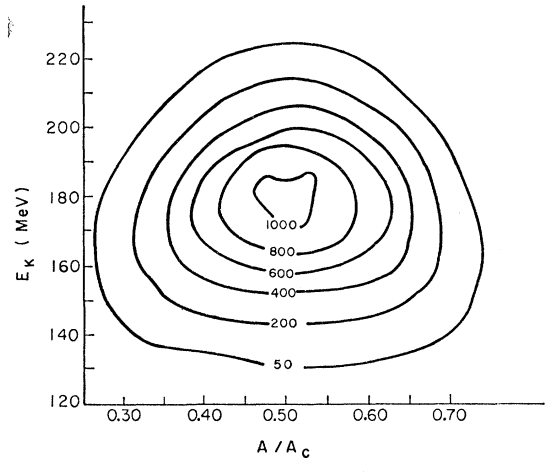

FIG. 4. Contour map in the coordinates A/A_c and E_K for O^{16}(138 MeV)+U^{238}.

[9] T. Sikkeland, E. L. Haines, and V. E. Viola, Phys. Rev. 125, 1350 (1962).

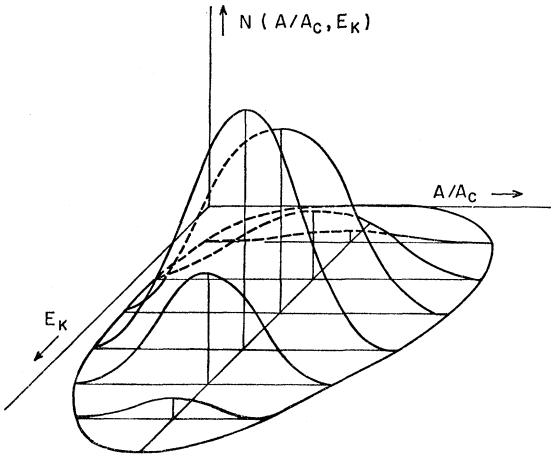

FIG. 5. Contour map for O^{16}(138 MeV)+U^{238} shown as mass distributions for various values of E_K.

We may think of the original data as being a three-dimensional surface, of which two coordinates are the two pulse heights, and the third is the density of events (a function of the two pulse heights). We shall refer to all such three-dimensional plots as "contour maps." It was shown above that two pulse-height coordinates may be transformed into mass and total-kinetic-energy coordinates, A/A_c and E_K, respectively. To form a contour map with mass-energy coordinates, we must also transform the density of events to the new coordinate system. Figure 4 shows an example of such a transformed mass-energy contour map.

We may consider a contour map with coordinates A/A_c and E_K to be a series of mass distributions changing with total kinetic energy (Fig. 5). Or it may be thought of as a series of total-kinetic-energy distributions changing with mass.[10]

B. Moments of the Mass Distribution

Each contour map was divided into a series of mass distributions in total-kinetic-energy intervals of 2 MeV. That is, each distribution represented all the events whose total kinetic energies lay between E_K-1 and E_K+1. For each distribution the second and fourth central moments were calculated.[11] The second and fourth central moments are

$$\mu_r(A/A_c) = \frac{\sum(A/A_c - \langle A/A_c\rangle)^r N(A/A_c)}{\sum N(A/A_c)},$$

where r equals 2 and 4, respectively, and $N(A/A_c)$ is the number of events in the distribution having mass

[10] H. C. Britt, H. E. Wegner, and Judith C. Gursky, Phys. Rev. 129, 2239 (1963).

[11] A. Hald, *Statistical Theory with Engineering Applications* (John Wiley & Sons, Inc., New York, 1952).

A/A_c. The mean of a mass distribution for a constant interval of E_K is

$$\langle A/A_c\rangle=\frac{\sum(A/A_c)N(A/A_c)}{\sum N(A/A_c)}.$$

These means showed only small excursions from a value of 0.5, as was expected.

The second central moment of any distribution is its variance. It provides a measure of the width of the distribution. The fourth central moment was used to calculate the coefficient of flatness,

$$\alpha_4=(\mu_4/\mu_2^2)-3.$$

This coefficient is zero for a Gaussian distribution and negative for a flat-topped distribution.

C. Treatment of Errors

Among the sources of uncertainty contributing to the dispersion of the mass distributions were electronic noise, the thickness of the targets, the width of the collimated detector, and the emission of neutrons from the excited fission fragments.[4] To a first approximation, any shifts in the mean values of the mass distributions due to these effects are zero or small. The contributions of the last three sources to the variances were calculated.[4,12] The contributions from target thickness and detector width were found to be negligible when compared with the contribution from neutron emission. The contribution of electronic noise was compared indirectly with that of neutron emission in the following manner. The fission-fragment mass distribution for the system C^{12}(112 MeV)+U^{238} was measured both radiochemically[13] and electronically. We assumed that the variance of the radiochemical mass distribution is unchanged by neutron emission. When corrected for the effects of neutron emission, the variance of the electronic mass distribution compared very well with that of the radiochemical. From this we concluded that the effects of electronic noise, and for that matter of all other sources of dispersion, are much smaller than the effects of neutron emission. Thus, the variances of the mass distributions were corrected only for the effects of neutron emission. No corrections were calculated for α_4, the coefficient of flatness.

Unlike the mass distributions, the total kinetic-energy distributions were subject to mean-value shifts as well as to dispersions. Thus, E_K was corrected for the mean-energy degradation in the target and the mean effects of neutron emission. Corrections for the dispersive effects of neutron emission slightly contracted the E_K distributions.

TABLE I. List of the reactions studied in these experiments, the excitation and rotational energies of the compound nuclei, and the slopes and intercepts, $\hat{E}_K$, of the plots of $\mu_2(A/A_c)$ versus E_K. The rotational energy is that of the spherical compound nucleus based on the maximum classical impact parameter.

Reaction	Excitation energy (MeV)	Upper limit of rotational energy (MeV)	Slope $[(A/A_c)^2$ $(\text{MeV})^{-1}]$ $(\times10^{-4})$	$\hat{E}_K$ (MeV)
C^{12}(124 MeV)+Pu^{242}	92	11.2	−0.77	249
O^{16}(165 MeV)+U^{238}	116	20.6	−1.00	247
O^{16}(158 MeV)+U^{238}	110	18.8	−1.18	247
O^{16}(141 MeV)+U^{238}	95	14.3	−1.04	255
O^{16}(138 MeV)+U^{238}	92	13.5	−1.04	248
O^{16}(138 MeV)+U^{238} [a]	92	13.5	−1.02	255
O^{16}(129 MeV)+U^{238}	83	11.2	−1.08	252
O^{16}(129 MeV)+U^{238} [a]	83	11.2	−0.77	248
O^{16}(103 MeV)+U^{238}	58	4.3	...	...
Ne^{22}(171 MeV)+Th^{232}	103	23.6	−1.01	259
Ne^{22}(137 MeV)+Th^{232}	72	11.3	−0.93	248

[a] Repeated experiments.

[12] See James Terrell, Phys. Rev. **127**, 880 (1962). See Appendix III therein.

IV. RESULTS

The first column in Table I lists all the reactions studied. The kinetic-energy and mass distributions are similar in all cases and have the general appearance illustrated in Fig. 5.

The most probable events are characterized by equal mass division and a kinetic energy of about 188 MeV. For mass divisions and kinetic energies deviating from the most probable values, the number of events decreases rapidly in a monotonic manner. Mass distributions for a fixed kinetic energy are bell-shaped and, with one exception, the widths of the mass distributions decrease markedly with increasing kinetic energy. We shall discuss this feature in detail.

Figures 6 through 9 show the variance of the mass distribution as a function of the kinetic energy for some

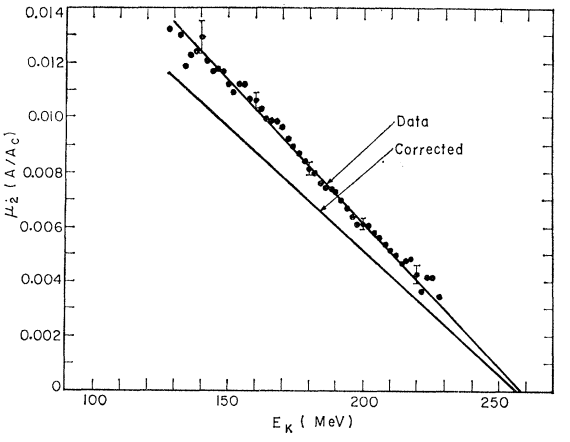

FIG. 6. Variance of the mass distribution versus E_K for O^{16}(138 MeV)+U^{238}. The lower curve shows the data corrected for the effects of neutron emission.

[13] Eldon L. Haines, Lawrence Radiation Laboratory Report UCRL-9566, 1961 (unpublished), p. 106.

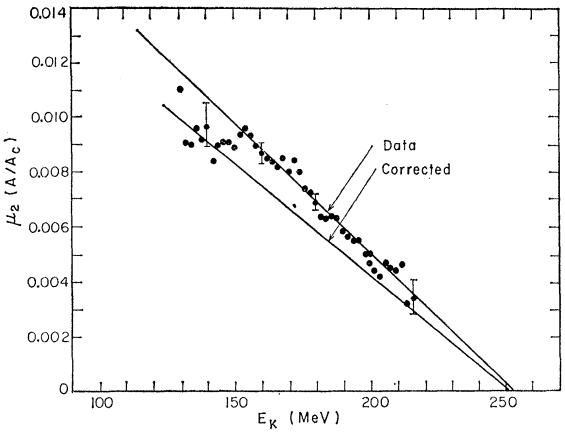

FIG. 7. Variance of the mass distribution versus E_K for Ne^{22}(137 MeV)+Th^{232}. The lower curve shows the data corrected for the effects of neutron emission.

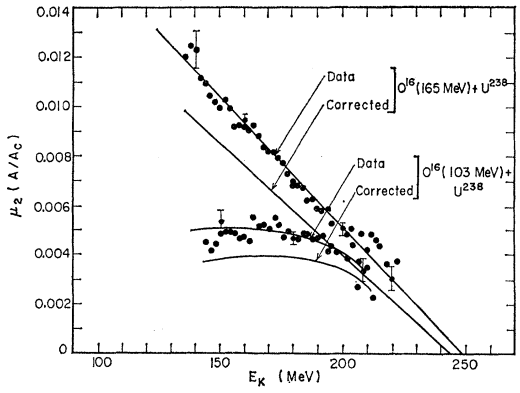

FIG. 9. Variance of the mass distributions versus E_K for the systems with highest and lowest excitation energies of these experiments (116 and 58 MeV). In each case the lower curve shows the data corrected for the effects of neutron emission.

of the experiments. We note that with the exception of the reaction O^{16}(103 MeV)+U^{238}, the variance (proportional to the *square* of the width of the mass distribution) decreases in a linear manner with increasing kinetic energy. A single straight-line relation seems to hold over the entire range of measurements from about 140 to 220 MeV. In this interval the variance decreases by a factor of 4. The slopes and intercepts of these lines are given in Table I. The case of O^{16}(103 MeV)+U^{238} constitutes a notable exception to the above behavior (Fig. 9). In this case the characteristic increase of the variance with decreasing kinetic energy does not hold below about 190 MeV. In fact, for low energies the variance appears to become independent of the energy.

In addition to the above over-all features of the kinetic-energy and mass distributions, which will be discussed in the next section, further characteristics are revealed by a more detailed analysis of the data. The mass distributions are almost Gaussian at the highest kinetic energy, but become gradually more nearly rectangular with decreasing energy. Figure 10 gives a quantitative description of this effect.

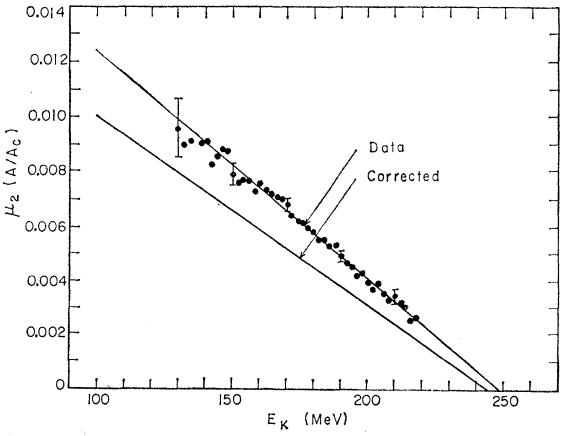

FIG. 8. Variance of the mass distribution versus E_K for C^{12}(124 MeV)+Pu^{242}. The lower curve shows the data corrected for the effects of neutron emission.

V. DISCUSSION

A. Mass Distributions

The systematic decrease of the variance of the mass distributions, illustrated in Figs. 6 through 9, may be associated with the loss of freedom of the fissioning nucleus to choose its asymmetry (at the moment of scission), as the restriction imposed by the requirement of a higher kinetic energy becomes more and more severe.[14] In the case of O^{16}(103 MeV)+U^{238}, for which the excitation energy is 58 MeV, the freedom to choose asymmetry does not continue to increase with decreasing kinetic energy (see Fig. 9). Because this was the only deviating case studied, we will not discuss it further than to point out the possible association between the rather constant restriction on the asymmetry

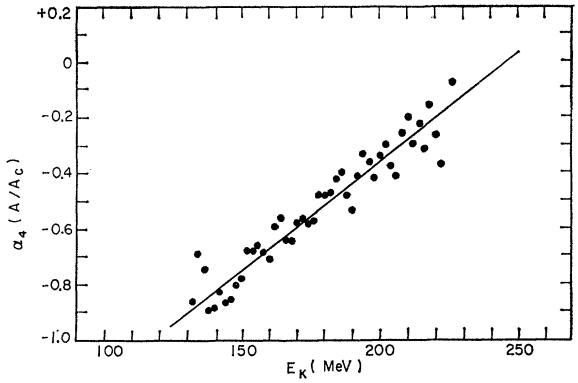

FIG. 10. Coefficient of flatness of the mass distributions versus E_K for O^{16}(138 MeV)+U^{238}. The lower the value of α_4, the more rectangular the distribution. For a Gaussian distribution, α_4 equals zero.

[14] Walter M. Gibson, Bell Telephone Laboratory (private communication).

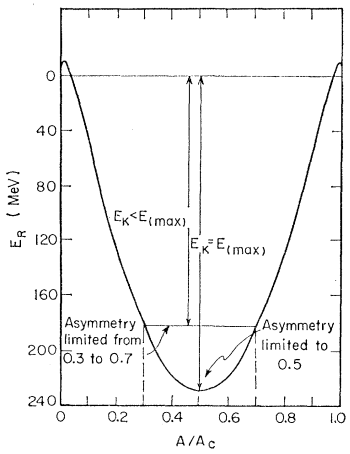

FIG. 11. Energy release as a function of mass for the spontaneous fission of Fm^{254}, illustrating the limits placed on the mass asymmetry for different E_K. The curve is based on the constant-charge-ratio hypothesis.

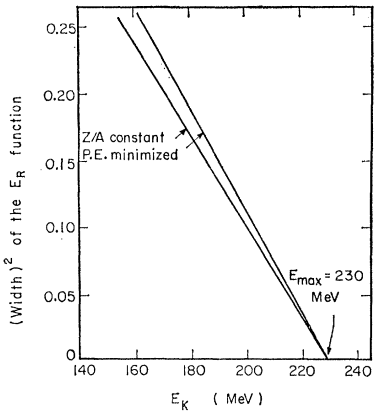

FIG. 12. The square of the width of the energy-release function, $(1-2A/A_c)^2$, versus E_K for Fm^{254}. The term, $1-2A/A_c$, represents the greatest asymmetry attainable for a given total kinetic energy, E_K.

at low kinetic energies and the relatively low excitation energy.

Since the maximum energy available for fission is always limited, an extreme situation would be realized in those cases in which all available energy is required to appear as kinetic energy. In such cases (where relative frequency would be increasingly small) there would be no energy left for deviations of any other variables from their optimum values (i.e., those values associated with the maximum energy release). Consequently, the variances of all distributions, including, in particular, the mass-division variable, would tend to zero as the kinetic energy approaches a certain upper limit. More generally, at any given kinetic energy an upper limit, required by conservation of energy, can be written on the value of any variable. We shall illustrate this in the case of the mass-division variable A/A_c. Figure 11 shows a plot of the energy release, E_R, for Fm^{254} as a function of A/A_c. According to the liquid-drop formula, used in this illustration, the maximum energy release $E_{max}=230$ MeV occurs for symmetric fission, and in the spontaneous fission of such a liquid drop, only strictly symmetric divisions would be energetically possible for events characterized by a kinetic energy release of $E_K=230$ MeV. Figure 11 shows that the range of asymmetries available energetically for a kinetic energy E_K smaller than this upper limit would be (approximately) proportional to the square root of $(E_{max}-E_K)$. In other words, the square of the maximum width of a mass-division distribution should be approximately a straight line in a plot against E_K. This is illustrated in Fig. 12.

We may compare this result with the empirical findings in Figs. 6 through 9 that the variance of the mass distributions—equal to the square of the rms widths—depends linearly on E_K. The slopes of the experimental lines are listed in Table I, as are the intercepts $\hat{E}_K$. All ten observed slopes are similar, and the intercepts are all quite close to 252 MeV (the average is 252 ± 4 MeV). We have estimated that in the spontaneous fission of Fm^{254} the maximum energy which could be released is about 230 MeV. This estimate is subject to some uncertainties. If we take into account the special stability of the two symmetric fragments, each with $Z=50$, (according to Cameron's masses) 243 MeV is found for the energy release. We may also point out that 252 MeV is equal to the potential energy of two equal spherical fragments whose centers are separated by 14.3 F, which corresponds to almost tangent spheres. Although this may have a deeper significance, we have not been able to find a convincing argument why the variance of the mass-division coordinate should tend to zero at kinetic energies corresponding to this particular configuration. The experimental value of about 252 MeV for the intercepts is near the maximum energy release. Although the intercept appears to be somewhat higher than the maximum energy release, there is of course no violation of energy conservation, since in the case of induced fission the total amount of energy available may be higher in fact, making E_{total} between 290 and 340 MeV. That the intercept $\hat{E}_K$ comes out closer to the energy release than the total energy is in line with the expectation that most of the extra energy, being in the form of internal excitation, is not easily available for conversion into kinetic energy of the fragments.

Estimating how much excitation energy is actually present in the nucleus at the moment of fission is difficult in general. We would like to conclude this discussion with a consideration of the factors that tend to make the relevant excitation energy different from that obtained from the Q value of the reaction.

B. Remarks Concerning the Excitation Energy

In some cases the heavy ion breaks apart and deposits only a fraction of its mass in the target nucleus. This leads to the formation of an excited nucleus which has not only a lower excitation energy, but also a lower mass and charge than the expected compound nucleus. If the resulting nucleus is very heavy, it will usually have sufficient energy to fission. Thus, events involving compound-nucleus formation may be mixed with fission events from nuclei of uncertain mass, charge, and excitation energy.

However, the linear velocities of the excited nuclei resulting from breakup reactions are lower than those of nuclei formed by the capture of the entire heavy ions. This forward velocity is given to the fission fragments. The two fragments from a low-velocity event (corresponding to breakup-induced fission) emerge in the laboratory system separated by larger angles than do two fragments from a high-velocity event (corresponding to heavy-ion-induced fission). This has been graphically illustrated by Sikkeland *et al.*[9] In the cases of the maximum energies of the heavy ions (10 MeV per nucleon), there is a large difference in the angles between the fission fragments produced by the two reactions. If the detectors are located to detect fragments from compound-nucleus fission, essentially no fragments from breakup-induced fission are detected. However, at lower bombarding energies there is a smaller difference in the angle between fragments produced in the two cases. Thus, at lower bombarding energies a larger fraction of the observed fragments come from breakup-induced fission. This fraction is estimated to be 5% for the reaction O^{16}(138 MeV)+U^{238}.

However, we may compare the results of two experiments, one in which the observed fragments came only from compound-nucleus fission, the other in which some of the fragments also came from fission following a breakup reaction. Figure 6 shows a plot of $\mu_2(A/A_c)$ versus E_K of the fragments for the reaction O^{16}(138 MeV)+U^{238}. Approximately 5% of the observed fragments came from breakup reactions. A comparison with a similar plot for the reaction O^{16}(165 MeV)+U^{238} (Fig. 9) reveals no apparent difference in shape. The slopes and intercepts are also not significantly different (see Table I). We may conclude that inclusion of some events of unknown initial mass, charge, and excitation energies has not significantly affected the widths of the distributions represented by $\mu_2(A/A_c)$ versus E_K.

For compound-nucleus reactions we must consider the distribution of total energy between excitation and rotation. We must also consider how much energy appeared in the form of neutrons before fission occurred. The calculated maximum rotational energies for spherical compound nuclei are listed in Table I for each case studied. In calculating these energies we assumed a spherical projectile colliding at a point just tangent to a spherical target. Such a collision gives the maximum rotational energy, which is probably more than twice the average energy. Thus, in the reaction with the highest rotational energy studied here, namely Ne^{22}(171 MeV)+Th^{232}, the average rotational energy is estimated to be about 10 MeV. During the fission process even this energy may be lower, because the moment of inertia becomes larger with increased distortion. In any event, even in this extreme case, the average rotational energy is less than or about 10% of the initial energy of the compound nucleus.

Angular momentum and rotational energy play an important role in the probability of partial de-excitation of the compound nucleus by neutron emission. Hiskes has shown that the fission barrier is lowered by large angular momentum.[15] The calculations of Pik-Pichak indicate that neutron emission is hindered by high angular momentum.[16] A study of the available experimental data by Vandenbosch and Huizenga showed that, for 1-MeV decrease in the difference between the fission threshold and the neutron binding energy, the average value of Γ_n/Γ_f decreases an order of magnitude.[17] The average experimental values of Γ_n/Γ_f for the reactions $Cf^{252}(\alpha,4n)Fm^{252}$ and $U^{238}(O^{16},4n)Fm^{250}$ are $\sim$0.25 and $\sim$0.07, respectively.[18,19] Although the excitation energies of comparable compound nuclei produced in our experiments with heavy ions were larger, the correspondingly increased angular momenta should have reduced the effective values of Γ_n/Γ_f still further. De-excitation by neutron emission would, therefore, seem to be negligible. However, it should be emphasized that the conclusions of the experiments do not depend to any important degree on the validity of the arguments concerning the extent of de-excitation.

ACKNOWLEDGMENTS

Wladyslaw J. Swiatecki deserves our deepest thanks for the fruitful discussions which made this work possible. We wish to thank Torbjørn Sikkeland, not only for the use of his fission chamber, but also for the many good discussions of the experimental aspects. Frequent and critical discussions with Harry R. Bowman, J. C. D. Milton, Donald S. Burnett, Reinhard Brandt, Franz Plasil, Victor E. Viola, and J. Rayford Nix were vital in crystallizing our ideas.

We especially appreciate the help of Leonard E. Gibson and William W. Goldsworthy with the electronic system and the help of Elwood Douglas with the two-dimensional analyzer.

We wish to thank Professor I. Perlman for his continued interest and support.

[15] John R. Hiskes, Lawrence Radiation Laboratory Report UCRL-9275, 1960 (unpublished).

[16] G. A. Pik-Pichak, Zh. Eksperim. i Teor. Fiz. **38**, 768 (1960) [translation: Soviet Phys.—JETP **11**, 557 (1960)].

[17] R. Vandenbosch and J. R. Huizenga, in *Proceedings of the Second International Conference on the Peaceful Uses of Atomic Energy, Geneva, 1958* (United Nations, New York, 1958), Vol. 15, p. 284.

[18] T. Sikkeland, S. Amiel, and S. G. Thompson, Lawrence Radiation Laboratory Report UCRL-8103 Rev., 1959 (unpublished).

[19] G. N. Flerov, in *Proceedings of the Conference on Reactions Between Complex Nuclei*, edited by A. Zucker, R. S. Livingston, and F. T. Howard, ORNL-2606, 1958 (unpublished), p. 384.

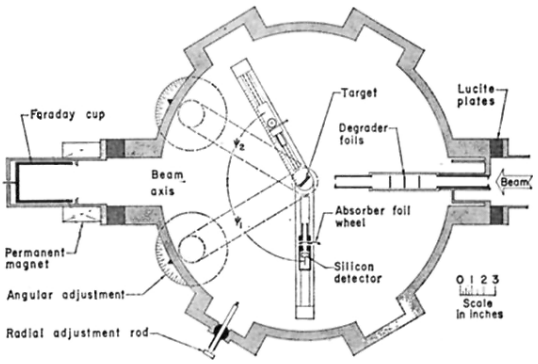

FIG. 1. Fission chamber. In the experiments described here, the detector located at angle ψ_2 was larger than that shown in the figure. Thus, it could detect all fission fragments in coincidence with those striking the detector at the angle ψ_1.